

Renormalized Flory-Huggins lattice model of mechanochemical kinetics and dynamic complexity in self-healing double-network hydrogel

Ziyu Xing¹, Mokarram Hossain² and Haibao Lu^{1,3}

¹Science and Technology on Advanced Composites in Special Environments Laboratory, Harbin Institute of Technology, Harbin 150080, China

²Zienkiewicz Centre for Computational Engineering, College of Engineering, Swansea University, Swansea, UK

³Corresponding author, E-mail: luhb@hit.edu.cn

Abstract: Double-network (DN) hydrogel exhibits high mechanical strength due to its reversibly mechanochemical transition and intrinsic self-healing reaction of dynamic bonds. In our study, a renormalized Flory-Huggins lattice model has been developed for the DN hydrogel, of which the mechanochemical kinetics and thermodynamics are originated from the stress-induced bond scission and entropic molecule rearrangement. A steric repulsive free-energy is firstly formulated to characterize the mechanochemical kinetics of bond scission. An extended free-energy model is then proposed for the extension and breakage of the newly formed bond in DN hydrogels, based on Gaussian distribution rule and Flory-Huggins theory. Finally, a variety of quantitative comparisons are conducted to identify the working mechanics with the experimental results, and the proposed model is able to provide a reliable metric for mechanochemical kinetics and dynamic complexity in the DN hydrogels.

Keywords: Double-network (DN) hydrogel; Flory-Huggins model; mechanochemical

1. Introduction

Inspired by nature, self-healing polymers have attracted great attention in various

applications ranging from biomedicines, civil structures, robots and aerospace.¹⁻⁴ Therefore, a huge effort has been made to enable the polymers with self-healing capabilities using various types of dynamic bonds, i.e., Diels-Alder (DA) cycloaddition, hydrogen bond and ionic bond, etc.⁵⁻⁷ These dynamic bonds have embedded into polymer chains to provide the self-healing ability in response to a suitable external stimulus, such as heat, light or chemistry.⁸⁻¹⁰

Hydrogel is one of the most popular polymeric soft matters, which have a wide range of tailorable properties. However, most hydrogels have low mechanical stiffness and strength because they do not have significant energy dissipation and self-healing abilities.¹¹ To overcome these drawbacks, the concept of double-network (DN) has been proposed for the hydrogels,¹²⁻¹⁹ in which the sacrificial bonds have been introduced to effectively dissipate the mechanical energy by means of mechanochemical transitions.²⁰⁻²⁶ It has been demonstrated that the fracture tensile stress and toughness of DN hydrogels have been significantly enhanced up to 10 MPa and 1000 J/m², respectively.¹⁶

To further improve the physical properties and self-healing abilities, reversible ionic bond,²⁷ hydrophobic association,²⁸ π - π stacking,²⁰ host-guest interaction²¹, and van der Waals force²² have been introduced into DN hydrogels to work as the sacrificial bonds²³. For self-healing DN hydrogels, the mechanochemical kinetics and dynamic complexity are essential for a full understanding of their constitutive relationship between molecular thermodynamics and macroscopic behavior. However, self-healing DN hydrogels normally undergo chemical reactions and complex interactions, i.e., bond scission, mechanochemical transition and molecule rearrangement. So far, few studies have been proposed to explore the working

mechanics and identify the constitutive relationship for the self-healing DN hydrogels.

2. Flory-Huggins lattice theory and free-energy equation

2.1 Steric repulsive free-energy equation

Under an external loading applied onto the DN hydrogel, the dynamic bonds in polymer chains could be broken, resulting in the increased number of chains. As shown in Figure 1, there are N_1 solvent molecules and N_2 polymer chains embedded in the Flory-Huggins lattice sites,²⁹⁻³¹ where the volume ratio of polymer chain to solvent molecule is x . Here, the lattice sites are $N=N_1+xN_2$. Each chain has a position probability of Z . A polymer chain (with a length of x) is broken into two chains with lengths of α and β , respectively.³³⁻³⁴ These newly formed chains are also governed by the Gaussian distribution theory.²⁹ Once the number of ways for arrangement (Ω) is known, the entropy ($S = k \ln \Omega$) can be obtained according to the Boltzmann principle.²⁹

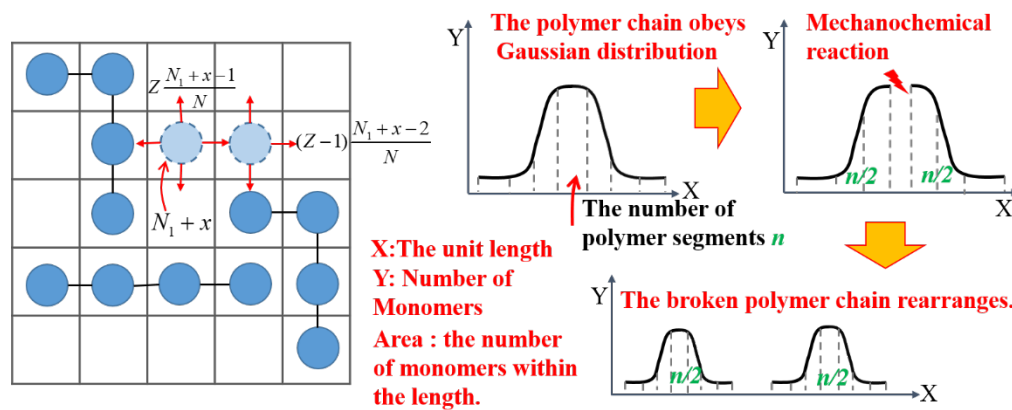


Figure 1. An illustration of Flory-Huggins lattice model for polymer chains immersed into a solvent, where there are mechanochemical reactions.

Initially, N_1 solvent molecules and N_2 polymer chains are set into the lattice sites,

and the total number of ways for arrangement is Ω . However, the broken chains are separated into two parts from the original ones, i.e., the first part occupies α sites, while the second one occupies β sites. The total number of ways to arrange the two parts are Ω_α and Ω_β , respectively,

$$\Omega = \frac{Z(Z-1)^{x-2}}{N^{x-1}} \prod_{i=1}^x (N_1 + i) \quad (1)$$

$$\begin{cases} \Omega_\alpha = \frac{Z(Z-1)^{x/2-2}}{N^{x/2-1}} \prod_{i=1}^{x/2} (N_1 + i + x/2) \\ \Omega_\beta = \frac{Z(Z-1)^{x/2-2}}{N^{x/2-1}} \prod_{i=1}^{x/2} (N_1 + i) \end{cases} \quad (2)$$

According to the Boltzmann principle,²⁹ the entropic change (ΔS_{cm}) is then written as:

$$\Delta S_{cm} = k_B \left(\ln \frac{\Omega_\alpha \Omega_\beta}{2} - \ln \Omega \right) = k_B \ln [Z(Z-1)^{-2} N] \quad (3)$$

where, k_B is a Boltzmann constant.

If N_{cm} of the polymer chains are involved into mechanochemical reaction, the mixing free energy (ΔF_M) can be expressed as,²⁹

$$\Delta F_M = -N_{cm} T k_B \ln \Omega = -N_{cm} T k_B \ln \frac{N}{x N_2} = N_{cm} T k_B \ln \phi_2 \quad (4)$$

According to the Gaussian distribution theory,²⁹ the probability of distribution (W) of polymer chain is,

$$W(x, y, z) = \left(\frac{B}{\sqrt{\pi}} \right)^3 e^{-B^2 h^2} \quad (5)$$

where, B represents the radial distribution parameter ($B^2 = \frac{3}{2h_0^2} = \frac{3}{2nb^2}$, h_0 is the initial end-to-end distance of a polymer chain, n is the number of monomers in a

polymer chain and b is the length of a monomer) and h is the end-to-end distance of a polymer chain.

The elastic free energy ($Q(h)$) is incorporated into the entropic function ($Q_C(h)$) and enthalpy function ($Q_E(h)$),^{30,31}

$$Q(h) = C_q \exp\left[\sum_{i=0}^{n-1} \ln\left(1 - i \frac{b^3}{h^3}\right)\right] \approx C_q \exp\left(-\frac{n^2 b^3}{2h^3}\right) \quad \left(\text{where } \frac{b^3}{h^3} \ll 1\right) \quad (6a)$$

$$Q_E(h) = C_e \exp\left(-\frac{E(h)}{k_B T}\right) = C_e \exp(-\chi n) \exp\left(\chi n^2 \frac{b^3}{h^3}\right) \quad (6b)$$

where, $E(h)$ is the activation energy, both C_q and C_e are given constants.

In combination of the Gaussian distribution theory and Flory-Huggins theory,²⁹⁻³¹ the number of ways for the newly formed polymer chains can be expressed as:

$$\Omega_{el} = W \times Q \times Q_E = C_{el} \exp\left[-\frac{3h^2}{2h_0^2} - \frac{n^{1/2} h_0^3}{2h^3} (1 - 2\chi)\right] \quad (7)$$

If we introduce rubber-elastic theory into equation (7),³¹ a constitutive relationship among elastic free energy (F_{el}), end-to-end distance (h) and number of monomer (n) in a polymer chain can be obtained as:

$$F_{el}(h, n) = N_{el} k_B T \frac{n^2 b^3}{2h^3} (1 - 2\chi) \quad (8)$$

where N_{el} is the number of polymer chains and χ is Huggins interactive parameter.

When each polymer chain is broken into two parts, the change in elastic free-energy

($\Delta F_{el}(n)$) can therefore be obtained as,

$$\Delta F_{el}(n) = F_{el}(h_0, n) - 2F_{el}\left(h_0, \frac{n}{2}\right) = k_B T \frac{n^2 b^3}{4h^3} (1 - 2\chi) \quad (9)$$

And then, the steric repulsive free-energy (ΔF_a) of the newly formed polymer chains is introduced,³²

$$\Delta F_a = k_B T \left(\frac{1}{2} - \chi \right) \frac{v^2 B^3 m^2}{V_1 \sqrt{2\pi^3}} e^{-B^2 a^2 / 2} \quad (10)$$

where, m is the molar weight of the original macromolecule and a is the steric distance between new two macromolecules, v is the molar volume ratio of polymer to solvent, and V_1 is the molar volume of polymer.

Here, there are N_{cm} number of polymer chains involved in the mechanochemical transition of the DN hydrogel. In combination of equations (9) and (10), the free-energy equation can be further expressed as,

$$\Delta F_{cm} = N_{cm} (\Delta F_{el}(n) + \Delta F_a) = N_{cm} k_B T \left(\frac{1}{2} - \chi \right) \left(\frac{n^2 b^3}{2h^3} + \frac{v^2 B^3 m^2}{V_1 \sqrt{2\pi^3}} e^{-(Bk_a)^2 (\lambda-1)^2 / 2} \right) \quad (11)$$

By substituting equations (4) and (9) into (11), the free-energy function can be finally obtained as,

$$\begin{aligned} \Delta F = \Delta F_{el}(h) - \Delta F_M - \Delta F_{cm} = k_B T \{ & -N_{cm} \ln \phi_2 + N_{el} \left[\frac{3}{2} \left(\frac{h^2}{h_0^2} - 1 \right) \right. \\ & \left. + \left(\frac{n^{1/2} h_0^3}{2h^3} - \frac{n^{1/2}}{2} \right) (1 - 2\chi) \right] - \bar{N}_{cm} \left(\frac{1}{2} - \chi \right) \left(\frac{n^2 b^3}{2h^3} + \frac{v^2 B^3 m^2}{V_1 \sqrt{2\pi^3}} e^{-(Bk_a)^2 (\lambda-1)^2 / 2} \right) \} \end{aligned} \quad (12)$$

2.2 Free-energy equation of mechanochemical kinetics

For the self-healing DN hydrogel, the mechanochemical reaction is reversible, as illustrated in [Figure 2](#). Two monomers are crosslinked by the dynamic bond in the polymer chains. Under an external force, the dynamic bond is broken resulting in two radicals of two monomers. Furthermore, the end-to-end distance of two monomers is further increased and is ruled by the Rouse diffusion motion³⁵⁻³⁸.

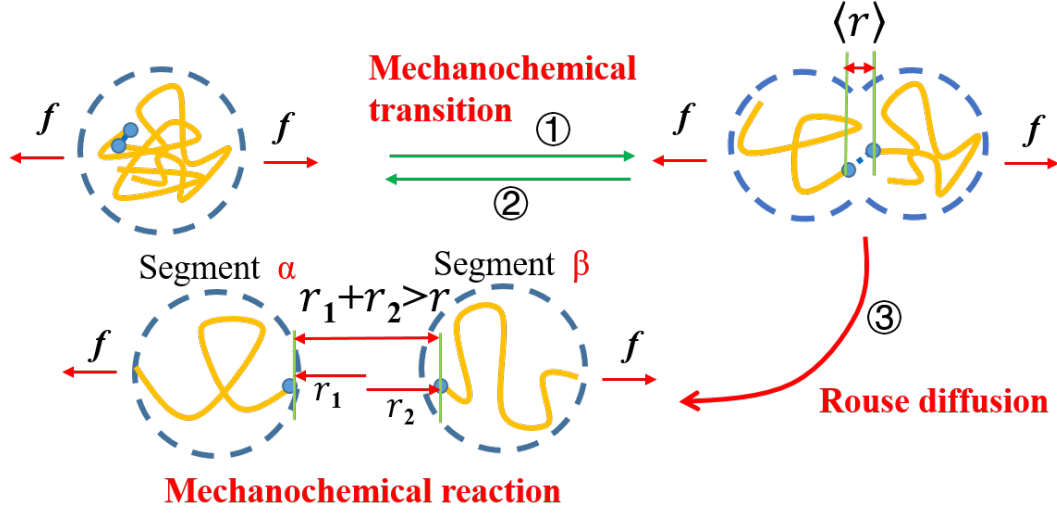


Figure 2. Schematic diagram of mechanochemical transition and Rouse diffusion of dynamic bond and monomers, respectively.

According to the theory of Rouse sub-diffusive motion,³⁵⁻³⁸ the reaction rate (k_1) is introduced to characterize the chemical kinetics that is governed by the Arrhenius formula,³⁹

$$k_1 = k_0 \exp\left(-\frac{E_a - k_f f}{k_B T}\right) \quad (13)$$

where, f is the force applied on polymer chains, E_a is the dissociation energy of dynamic bond, both k_f and k_0 are given material constants.

The length of the newly formed polymer chain (j) can be expressed as,^{33,34}

$$j = j_0 \exp\left(\frac{-k_f f}{2k_B T}\right) \quad (14)$$

where, j_0 is the initial length of a virginal chain, when $f = 0$.

Here, it is assumed that there are N_{cm} chains involved in the mechanochemical transition which can be expressed using,

$$N_{cm} \equiv N_0 \left(\frac{j_0}{j} - 1 \right) = N_0 \left[\exp\left(\frac{k_f f}{2k_B T}\right) - 1 \right] \quad (15)$$

where, N_0 is a given constant.

According to the rubber-elastic theory,³¹ we can obtain,

$$f = \frac{3k_B T}{nb^2} h \quad (16a)$$

$$h_0^2 = nb^2 = \lambda_0^2 = 1 \quad \text{and} \quad B^2 = \frac{3}{2h_0^2} = \frac{3}{2} \quad (16b)$$

$$h = \sqrt{\lambda_x^2 + \lambda_y^2 + \lambda_z^2} = \sqrt{\lambda^2 + \frac{2}{\lambda}} \quad \left(\lambda_x = \lambda \quad \text{and} \quad \lambda_y = \lambda_z = \frac{1}{\sqrt{\lambda}} \right) \quad (16c)$$

where, λ_0 and λ are the initial and final stretching ratios, respectively.

By substituting equation (16a) into (15), we can obtain the following equation:

$$N_{cm} = N_0 \left[\exp\left(\frac{k_f h}{2nb^2}\right) - 1 \right] \quad (17)$$

In combination of equations (12), (16) and (17), the free-energy function is obtained,

$$\begin{aligned} \Delta F = & k_B T \left\{ N_0 \left[\exp\left(\frac{k_f h}{2h_0^2}\right) - 1 \right] \ln \frac{1}{\phi_2} + N_{el} \left[\frac{3}{2} \left(\frac{h^2}{h_0^2} - 1 \right) + \left(\frac{n^{1/2} h_0^3}{2h^3} - \frac{n^{1/2}}{2} \right) (1 - 2\chi) \right] \right. \\ & \left. - \bar{N}_{cm} \left(\frac{1}{2} - \chi \right) \left(\frac{n^{1/2} h_0^3}{2h^3} + \frac{v^2}{V_1} \frac{B^3 m^2}{\sqrt{2\pi^3}} e^{-(Bk_a)^2 (\lambda-1)^2 / 2} \right) \right\} \quad (18a) \end{aligned}$$

$$\begin{aligned} \Delta F = & k_B T \left\{ N_0 \left[\exp\left(\frac{k_f \sqrt{\lambda^2 + \frac{2}{\lambda}}}{2}\right) - 1 \right] \ln \frac{1}{\phi_2} + N_{el} \frac{3}{2} \left(\lambda^2 + \frac{2}{\lambda} - 1 \right) - N_{ta} \frac{1}{3 \left(\lambda^2 + \frac{2}{\lambda} \right)^{3/2}} \right. \\ & \left. + N_{el} \frac{n^{1/2}}{2} (1 - 2\chi) - \frac{1}{2} \bar{N}_{cm} \left(\frac{1}{2} - \chi \right) \frac{v^2}{V_1} \frac{27m^2}{4\sqrt{2\pi^3}} \exp\left[-\frac{9k_a^2}{8} (\lambda - 1)^2\right] \right\} \quad (18b) \end{aligned}$$

where, $N_{ta} = \left(\frac{3\bar{N}_{cm}}{2} - 3N_{el} \right) (1 - 2\chi) n^{1/2}$. Therefore, the constitutive relationship of

stress as a function of stretching ratio can be expressed as follows,

$$\begin{aligned}
\sigma = \frac{\partial \Delta F}{\partial \lambda} = & k_B T \left\{ \frac{N_0 k_f \ln\left(\frac{1}{\phi_2}\right) \left(\lambda - \frac{1}{\lambda^2}\right)}{2\sqrt{\lambda^2 + \frac{2}{\lambda}}} \exp\left(\frac{k_f \sqrt{\lambda^2 + \frac{2}{\lambda}}}{2}\right) + 3N_{el} \left(\lambda - \frac{1}{\lambda^2}\right) \right. \\
& + \bar{N}_{cm} \left(\frac{1}{2} - \chi\right) \frac{v^2}{V_1} \frac{27m^2}{4\sqrt{2\pi^3}} \frac{9k_a^2}{8} (\lambda - 1) \exp\left[-\frac{9k_a^2}{8} (\lambda - 1)^2\right] \\
& \left. + \left(\frac{3\bar{N}_{cm}}{2} - 3N_{el}\right) (1 - 2\chi) n^{1/2} \frac{\left(\lambda - \frac{1}{\lambda^2}\right)}{\left(\lambda^2 + \frac{2}{\lambda}\right)^{5/2}} \right\} \quad (19)
\end{aligned}$$

If the broken probability of dynamic bond is estimated by the Boltzmann function

$$f_a = \exp\left(-\frac{\Delta F_a}{k_B T}\right),$$

the repulsive volume is then obtained as,

$$V_r = \int_0^\infty (1 - f_a) 4\pi a^2 da = 2\pi^2 \int_0^\infty [1 - \exp\left(\left(\chi - \frac{1}{2}\right) \frac{v^2}{V_1} \frac{B^3 m^2}{\sqrt{2\pi^3}} e^{-B^2 a^2 / 2}\right)] a^2 da \quad (20)$$

Based the equations (10) and (20), the stress-strain relationship of repulsive free energy can therefore be obtained:

$$\begin{aligned}
\sigma_a = \frac{\partial \Delta F_a}{\partial \lambda} = & \frac{\partial \Delta F_a}{\partial V_r} \frac{\partial V_r}{\partial \lambda} = \frac{N^a k_B T k_a e^{-B^2 a^2 / 2} [1 - \exp\left(\left(\chi - \frac{1}{2}\right) \frac{v^2}{V_1} \frac{B^3 m^2}{\sqrt{2\pi^3}} e^{-B^2 a^2 / 2}\right)] a^2}{\int_0^\infty \exp\left[\left(\chi - \frac{1}{2}\right) \frac{v^2}{V_1} \frac{B^3 m^2}{\sqrt{2\pi^3}} e^{-B^2 a^2 / 2} - B^2 a^2 / 2\right] a^2 da} \quad (21)
\end{aligned}$$

where, a is the distance between two DN hydrogel networks, which is estimated as

$a = k_a (\lambda - 1)$. In combination of equations (4), (8), and (21), the constitutive stress-strain relationship of the DN hydrogel is finally obtained:

$$\begin{aligned}
\sigma = \sigma_M + \sigma_{el} - \sigma_a = & RT \left[n_{el} \left(\frac{\lambda}{\lambda_0^2} - \frac{\lambda_0}{\lambda^2} \right) - \right. \\
& \left. C_a e^{-(Bk_a(\lambda-1))^2 / 2} [1 - \exp\left(\left(\chi - \frac{1}{2}\right) \frac{v^2}{V_1} \frac{B^3 m^2}{\sqrt{2\pi^3}} e^{-(Bk_a(\lambda-1))^2 / 2}\right)] (\lambda - 1)^2 \right] + L \quad (22)
\end{aligned}$$

where,
$$C_a = \frac{n_a k_a^3}{\int_0^\infty \exp[(\chi - \frac{1}{2}) \frac{v^2}{V_1} \frac{B^3 m^2}{\sqrt{2\pi^3}} e^{-B^2 a^2 / 2} - B^2 a^2 / 2] a^2 da}$$
 and L is a normalized parameter.

Based on the equations (19) and (20), the constitutive relationship between stress and elongation ratio is plotted in Figure 3, where the parameters used in equations

(19) and (20) are $N_{ei} k_B T \frac{n^{1/2}}{2} (1 - 2\chi) = 1.0 \text{ J}$, $N_0 k_B T \ln(\frac{1}{\phi_2}) = 0.5 \text{ MPa}$, $k_f = 0.4$, $3N_{ei} k_B T$

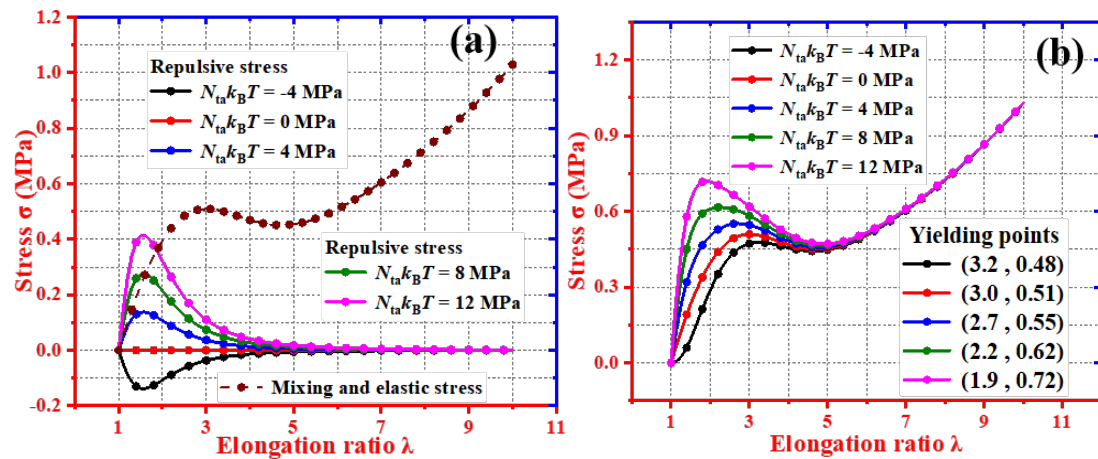
$= 0.03 \text{ MPa}$, $\bar{N}_{cm} k_B T = 1.5 \text{ MPa}$ and $\frac{9k_a^2}{8} = 0.2$. Figure 3(a) plots the analytical results of repulsive stress as a function of elongation ratio. It revealed that the repulsive stress is initially increased with an increase in the elongation ratio, and then it turns to decrease with a further increase in the elongation ratio. As shown in Figure 3(b), the yielding stress is increased from $\sigma = 0.48 \text{ MPa}$, $\sigma = 0.51 \text{ MPa}$, $\sigma = 0.55 \text{ MPa}$, $\sigma = 0.62$

MPa to $\sigma = 0.72 \text{ MPa}$ with an increase of $N_{ia} k_B T$ from -4 MPa to 12 MPa . These

analytical results reveal that a large amount of polymer chains have been involved in

the mechanochemical transitions (e.g., increases in $N_{ia} k_B T$ (or N_{ia})), resulting in

both repulsive and yielding stresses increased.



Figures 3. (a) Simulation results of repulsive stress as a function of elongation ratio for the DN hydrogel. (b) Simulation results of yielding stress as a function of elongation ratio for the DN hydrogel.

3. Experimental verification of mechanical behavior of DN hydrogel

Figure 4 plots theoretical and experimental results of mechanical stress at a variety of molar concentrations of PNaAMPS (poly(2-acrylamido-2-methylpropanesulfonic acid sodium salt) in PNaAMPS/PEA (PEA, poly(ethyl acrylate)) DN hydrogels. The parameters used are listed in Table 1. It is found that the theoretical results fit well with the experimental data¹⁸ of DN hydrogels with molar concentration of PNaAMPS network, whereas $x=2$ mol%, 3 mol%, 4 mol%, and 6 mol%. With an increase in the molar concentration of PNaAMPS network, the yielding stress is increased from 1.18 MPa, 2.03 MPa, 2.95 MPa to 4.75 MPa. In the DN hydrogels, the PNaAMPS network undergoes a mechanochemical transition in response to an external loading, while the PEA network is to resist an external loading by means of a mechanical stretching. Therefore, a larger amount of mechanical energy is used for mechanochemical transition than that is for the mechanical stretching.^{2,18} An increase in the molar concentration of the PNaAMPS network results in an increase in the mechanical energy, which is used for mechanochemical transition to be dissipated into the mechanical energy. Therefore, the mechanical strength is enhanced.

Table 1. Values of parameters used in equations (19) for PNaAMPS/PEA DN hydrogels with various cross-linker concentrations of the PEA network.

$x(\text{mol}\%)$	$N_0 k_B T \ln\left(\frac{1}{\phi_2}\right)$	k_f	$N_{ta} k_B T$	$3N_{el} k_B T$	$\bar{N}_{cm} k_B T$	$\frac{9k_a^2}{8}$
2	2.29	0.21	-8	0.05	6.67	0.03

3	3.71	0.21	-12	0.058	14	0.03
4	13.11	0.148	-15	0.06	15	0.05
6	22.13	0.16	-30	0.06	22	0.05

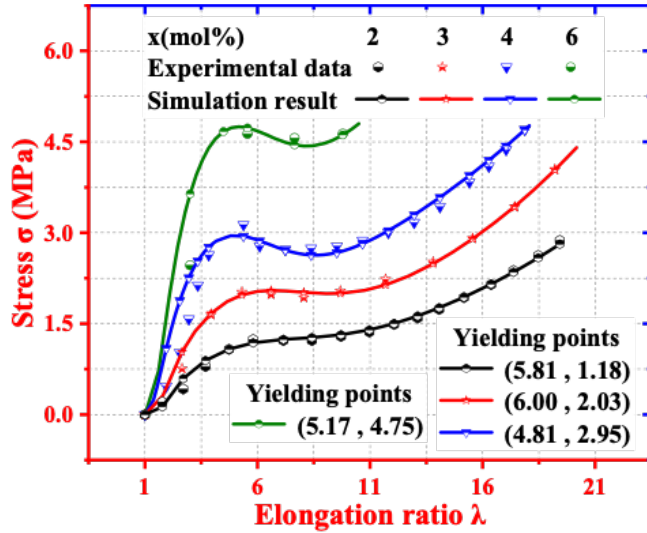


Figure 4. Comparison of simulation results and experimental data¹⁸ for the stress as a function of elongation ratio of PNaAMPS/PEA DN hydrogels with a variety of cross-linker concentration of the PEA network.

Meanwhile, four groups of experimental data from Ref. 40 of DN0.1, PVA-DN0.1, DN0.6, and PVA-DN0.6 hydrogels, which were synthesized from PVA/PAMPS/PAAm (PVA, poly(vinyl alcohol); PAAm, poly-acrylamide), have been employed to compare with the analytical results, where 0.1 or 0.6 mol% of 2-oxoglutaric acid has been used as the photoinitiator. The analytical and experimental results are both plotted in Figure 5, and the parameters used in calculation using the equation (19) are listed in Table 2. It is revealed that the yielding stresses are 0.77 MPa to 0.62 MPa for the DN0.1 and PVA-DN0.1 hydrogels, respectively, whereas those are 0.72 MPa and 0.46 MPa for the DN0.6 and PVA-DN0.6 hydrogels, respectively. After the PVA network is embedded into the DN hydrogels, the yielding stress is decreased. These analytical results are in good agreements with the experimental ones.⁴⁰ It is revealed

that the proposed model can be used to predict the mechanical behavior of DN and triple-network hydrogels.

Table 2. Values of parameters used in equations (19) for the yielding stress of DN and PVA-DN hydrogels with 0.1 mol% and 0.6 mol% of 2-oxoglutaric acid photoinitiator.

	$N_0 k_B T \ln\left(\frac{1}{\phi_2}\right)$	k_f	$N_{ia} k_B T$	$3N_{el} k_B T$	$\bar{N}'_{cm} k_B T$	$\frac{9k_a^2}{8}$
DN0.1	4.43	0.14	-4	0.03	2.38	0.08
PVA-DN0.1	3	0.16	-4	0.026	2.86	0.07
DN0.6	2.78	0.18	-4	0.022	1.63	0.08
PVA-DN0.6	1.87	0.15	-2	0.03	1.44	0.09

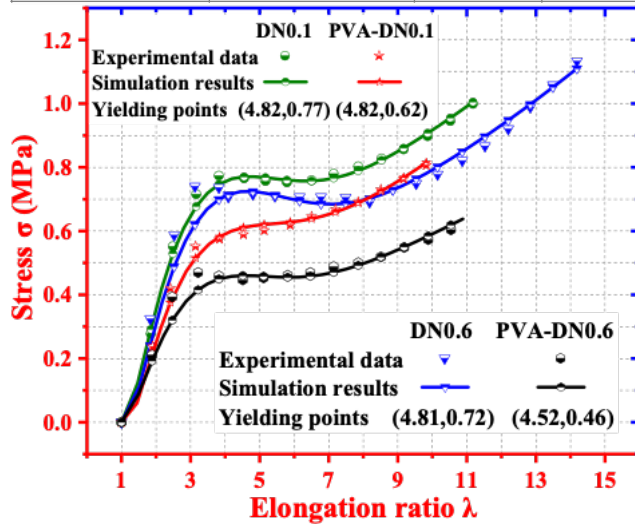


Figure 5. Comparisons of simulation results and experimental data⁴⁰ for the yielding stress as a function of elongation ratio of DN and PVA-DN hydrogels with 0.1 mol% and 0.6 mol% of 2-oxoglutaric acid photoinitiator.

Finally, the effect of molar fractions of network component on the mechanical property of DN hydrogels has been studied using our proposed model. Here, three groups of experimental data (reported in Ref. 41) of UM/NBOC (poly(ureidoethyl methacrylate (UM), nitrobenzyloxycarbonylaminoethyl methacrylate (NBOC)) DN hydrogels with a variety of molar fractions of NBOC network (e.g., $f_{\text{NBOC}} = 0.1, 0.15$

and 0.2), have been employed to verify the proposed model. All parameters used in the model are listed in Table 3. As revealed in Figure 6, the yielding stress is significantly increased from 0.11 MPa to 0.35 MPa with an increase of molar fraction of the NBOC network from 0.1 mol% to 0.2 mol%. The analytical and experimental results are in well agreements with each other. Here, the NBOC network is worked as the dynamic cross-linkers and enables the DN hydrogel stretchable. Therefore, the yielding strength is significantly enhanced due to the dynamic crosslinking of NBOC network, which dissipates the mechanical energy by means of mechanochemical transitions. On the other hand, the NBOC network can also reform polymerization, resulting in the self-healing of DN hydrogels and recovery of the yielding strength.

Table 3. Values of parameters used in equations (19) for different molar fraction $f_{\text{NBOC}} = 0.1, 0.15$ and 0.2 .

f_{NBOC}	$N_0 k_B T \ln\left(\frac{1}{\phi_2}\right)$	k_f	$N_{ta} k_B T$	$3N_{el} k_B T$	$\bar{N}_{cm} k_B T$	$\frac{9k_a^2}{8}$
0.1	0.175	0.48	1	0.009	0.22	0.09
0.15	0.313	0.48	3	0.02	0.44	
0.2	0.263	0.8	4	0.033	0.22	

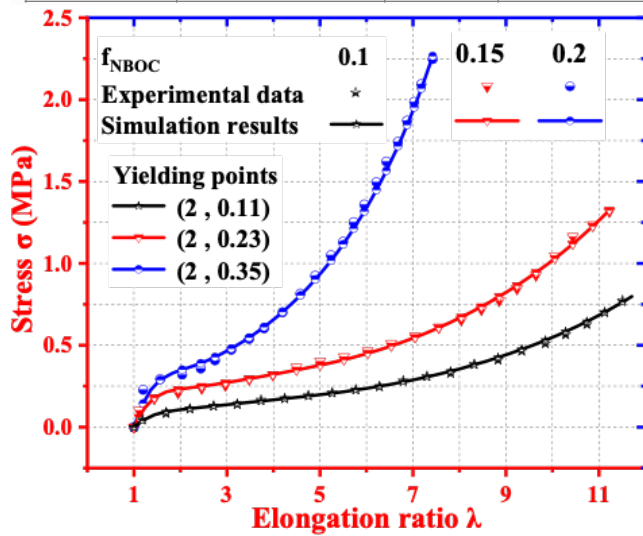


Figure 6. Comparisons between numerical results using equation (19) and experimental data reported in Ref. 41 of the UM/NBOC hydrogels at a variety of molar fractions of the NBOC network of $f_{\text{NBOC}}=0.1, 0.15$ and 0.2 .

To verify the proposed model further, the effect of water concentration ($1-\frac{1}{\lambda^3}$) on the nominal stress was investigated for the DN hydrogel, of which the mechanical behavior is critically determined by the swelling ratio (λ^3-1) according to the rubber-elastic theory.³¹ **Figure 7** plots the analytical results of nominal stress as a function of the tensile strain (λ) for DN hydrogel with various water concentrations. The values of parameters used in equation (23) have been collected in **Table 4**. It is found that the simulation results fit well with the experimental data of PDGI/PAAM (PDGI: poly(dodecyl glyceryl itaconate), PAAM: polyacrylamide) DN hydrogels with various water concentrations of 46%, 61%, 79%, 85% and 94%.⁴² With an increase in the water concentration, the yielding stress is gradually decreased from 0.60 MPa, 0.18 MPa, 0.17 MPa, 0.16 MPa to 0.05 MPa. That is to say, the yielding stress is gradually decreased with an increase in the water concentration ($1-\frac{1}{\lambda^3}$) and swelling ratio (λ^3-1), whereas these analytical and experimental results are coincident with the rubber-elastic theory.³¹

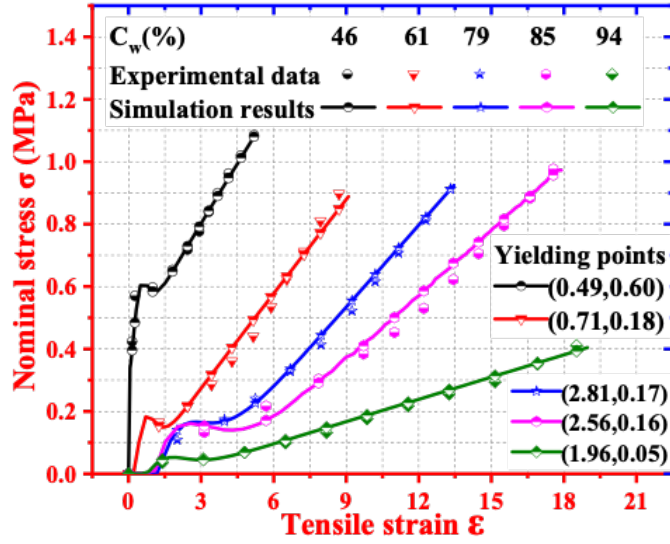


Figure 7. The comparison of simulation results and experimental data⁴² for the nominal stress as a function of tensile strain of DN hydrogel with various water concentrations.

Table 4. Values of parameters used in equations (23) for DN hydrogels incorporated

of various water concentrations, where $(\chi - \frac{1}{2}) \frac{v^2 B^3 m^2}{V_1 \sqrt{2\pi^3}} = 5.4$.

water concentration	n_{el}	C_a	Bk_a	L
46%	0.05	0.0035	1.2	0.31
61%	0.04	0.002	0.9	-0.12
79%	0.035	0.0003	0.3	-0.34
85%	0.028	0.00024	0.25	-0.35
94%	0.0095	0.00015	0.4	-0.07

Finally, the proposed model is used to characterize the mechanically cyclic stress of the PMPTC/PNaSS (PMPTC: poly(3-(methacryloylamino) propyl-trimethylammonium chloride); PNaSS: poly(p-styrene sulfonic acid sodium salt)) DN hydrogels. Figure 8 plots the analytical results of mechanical stress as a function of strain and the experimental data in Ref. 43 have been employed for verification. The parameters used for the loading processes have been listed in Table 5. Figure 8(a)

plots the stress-strain curve of PMPTC/PNaSS DN hydrogel performed by cyclic tensile tests. These analytical results fit well with the experimental data. Furthermore, it is revealed that the recovery performance of the DN hydrogel is significantly improved with an increase in waiting time from 0.5 min to 30 min. That is to say, the self-healing property of the PMPTC/PNaSS DN hydrogel can be well characterized by the proposed model. On the other hand, Figure 8(b) has been further presented to characterize the recovery behavior of DN hydrogel in the cyclically loading-unloading process. It should be noted that the unloading process is governed by the different equation in comparison with that of the loading process, owing to the difference in the chemical kinetics of bond breakage and the self-healing. The parameters used for the unloading processes are $C_a = 0.054$, $Bk_a = 0.2$, $(\chi - \frac{1}{2}) \frac{v^2 B^3 m^2}{V_1 \sqrt{2\pi^3}} = 2$ and $RT = 2.5 \times 10^3$ J/mol. With an increase in the waiting time from 0.5 min to 10 min, the λ_p is increased from 2.1 to 2.3, where it is $\lambda_p = 1.95$ in the first loading process. After a comparison, it is revealed that the analytical results of the proposed model can well predict the both loading and unloading processes of the self-healing DN hydrogel.

Table 5. The parameters used in equation (23) for the loading processes of PMPTC/PNaSS DN hydrogel.

	λ_p	n_{el}	C_a	Bk_a	$(\chi - \frac{1}{2}) \frac{v^2 B^3 m^2}{V_1 \sqrt{2\pi^3}}$	L
First loading	0	0.047	0.0021	1	5.7	0.45
0.5min	1.4	0.059	0.0012	1.2	5.4	0.075
2min	1.0	0.05	0.0012	1.2	5.4	0.16

5min	0.75	0.046	0.0018	1.2	5.4	0.23
10min	0.5	0.038	0.0015	1.1	5.4	0.34
30min	0.2	0.042	0.0025	1.1	5.4	0.43

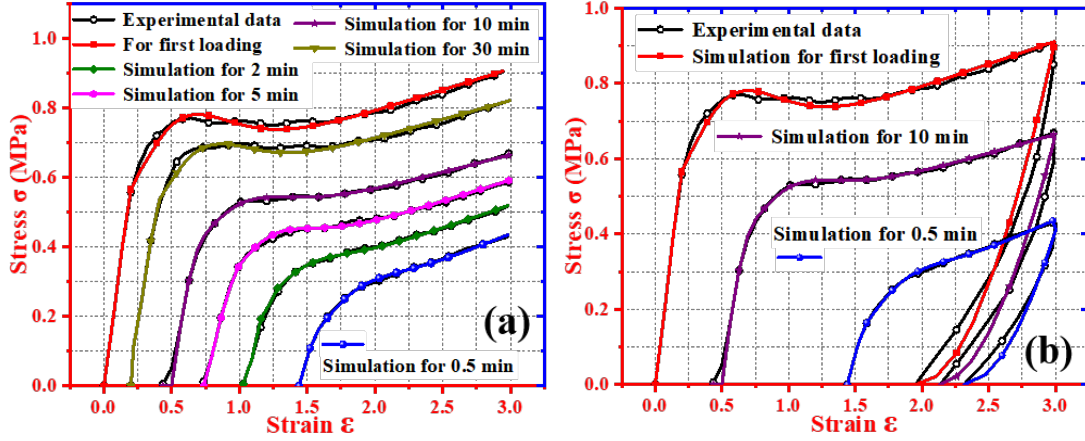


Figure 8. Recovery of the stress-strain curve for various waiting times performed by cyclic tensile test. (a) With the waiting time of 0.5 min, 2 min, 5 min, 10 min and 30 min. (b) With the waiting time of 0.5 min and 10 min.

4. Conclusions

Based on the renormalized Flory-Huggins lattice theory and Gaussian distribution rule, we propose a free energy-based model to describe the entropic molecule rearrangement and bond scission in DN hydrogels, in which two types of networks synchronously undergo mechanical extensions and mechanochemical transitions. A series of experimental results have been employed to identify the working principles and critical factors, i.e., mechanochemical transition, molar concentration, on the mechanical and yielding behaviors of DN hydrogels. Results demonstrate that the proposed model is able to characterize and predict mechanical behavior of DN hydrogels. Furthermore, our proposed model provides an effective methodology to investigate the mechanochemical kinetics and dynamic complexity, which are the

working principles to determine the mechanical properties of DN hydrogels undergoing self-healing bond scissions. Finally, the newly proposed model have been verified by the experimental results reported in the literature.

Acknowledgements

This work was financially supported by the National Natural Science Foundation of China (NSFC) under Grant No. 11672342 and 11725208.

References

- ¹B. J. Blaiszik, S. L. B. Kramer, S. C. Olugebefola, J. S. Moore, N. R. Sottos and S. R. White, [Annu. Rev. Mater. Res.](#) **40**, 179 (2010).
- ²T. Matsuda, R. Kawakami, R. Namba, T. Nakajima, and J. P. Gong, [Science](#) **363**, 504 (2019).
- ³H. B. Lu, W. M. Huang, X. L. Wu, Y. C. Ge, F. Zhang, and Zhao Y, [Smart Mater. Struct.](#) **23**, 067002 (2014).
- ⁴H. B. Lu, X. D. Wang, K. Yu, Y. Q. Fu, and J. S. Leng, [Smart Mater. Struct.](#) **28**, 025031 (2019).
- ⁵J. Hentschel, A. M. Kushner, J. Ziller, and Z. B. Guan, [Angew. Chem. Int. Edit.](#) **51**, 10561 (2012).
- ⁶F. Herbst, D. Döhler, P. Michael, and W. H. Binder, [Macromol. Rapid Comm.](#) **3**, 197 (2013).
- ⁷Y. L. Liu and T. W. Chuo, [Polym. Chem.](#) **4**, 2194 (2013).
- ⁸S. Billiet, X. K. D. Hillewaere, R. F. A. Teixeira, and F. E. D. Prez, [Macromol. Rapid Comm.](#) **4**, 290 (2012).

- ⁹P. Froimowicz, H. Frey, and K. Landfester, [Macromol. Rapid Comm.](#) **5**, 468 (2011).
- ¹⁰B. J. Adzima, C. J. Kloxin, and C. N. Bowman, [Adv. Mater.](#) **25**, 2784 (2010).
- ¹¹H. W. Yuk, T. Zhang, S. T. Lin, G. A. Parada, and X. H. Zhao, [Nat. Mater.](#) **15**, 190 (2016).
- ¹²R. Fuhrer, E. K. Athanassiou, N. A. Luechinger, and W. J. Stark, [Small](#) **5**, 383 (2009).
- ¹³W. J. Zheng, N. An, J. H. Yang, J. X. Zhou, and Y. M. Chen, [ACS Appl. Mater. Inter.](#) **7**, 1758 (2015).
- ¹⁴R. E. Webber, C. Creton, H. R. Brown, and J. P. Gong, [Macromolecules](#) **40**, 2919 (2007).
- ¹⁵S. S. Jang, W. A. Goddard, and M. Y. S. Kalani, [J. Phys. Chem. B](#) **111**, 1729 (2007).
- ¹⁶H. J. Kwon, K. Yasuda, Y. Ohmiya, K. Honma, Y. M. Chen, and J. P. Gong, [Acta Biomater.](#) **6**, 494 (2010).
- ¹⁷J. P. Gong, Y. Katsuyama, T. Kurokawa, and Y. Osada, [Adv. Mater.](#) **15**, 1155 (2003).
- ¹⁸T. Matsuda, T. Nakajima, and J. P. Gong, [Chem. Mater.](#) **31**, 3766 (2019).
- ¹⁹J. P. Gong, [Soft Matter](#) **6**, 2583 (2010).
- ²⁰Y. J. Zhao, K. Y. Zhao, Y. Li, L. Liu, X. X. Zhang, J. G. Li, M. Chen, and X. L. Wang, [Sci. China Technol. SC.](#) **61**, 438 (2018).
- ²¹H. B. Lu, X. J. Shi, K. Yu, and Y. Q. Fu, [Compos. Part B-Eng.](#) **165**, 456 (2019).
- ²²M. C. Koetting and J. T. Peters, [Mat. Sci. Eng. R](#) **93**, 1 (2015).
- ²³W. Hong, X. H. Zhao, and Z. G. Suo, [J. Mech. Phys. Solids](#) **58**, 558 (2010).
- ²⁴R. Marcombe and S. Q. Cai, [Soft Matter](#) **6**, 784 (2010).
- ²⁵J. Y. Li, Z. G. Suo, and J. J. Vlassak, [Soft Matter](#) **10**, 2582 (2014).
- ²⁶D. Basak and S. Ghosh, [ACS Macro Lett.](#) **2**, 799 (2013).

- ²⁷ Y. F. Yue, X. F. Li, T. Kurokawa, and J. P. Gong, *J. Mater. Chem. B.* **4**, 4104 (2016).
- ²⁸ S. J. Szheng, Z. Q. Li, and Z. S. Liu, *Sci. China Technol. SC.* **62**, 1375 (2019).
- ²⁹ M. J. He, H. D. Zhang, W. X. Chen, and X. X. Dong, *Polymer physics* (Shanghai: Fudan 2006)
- ³⁰ P. G. Gennes, *Scaling concepts in polymer physics* (Ithaca and London :Cornell University 1979)
- ³¹ L. R. G. Treloar, *The physics of rubber elasticity* (New York: Oxford University 1975)
- ³² Y. Q. Hua and R. G. Jin, *Polymer physics* (Beijing: Chemical industry 2013)
- ³³ K. B. Martin and C. S. Hauke, *Chem. Rev.* **105**, 2921 (2005).
- ³⁴ M. M. Caruso, D. A. Davis, Q. Shen, S. A. Odom, N. R. Sottos, S. R. White, and J. S. Moore, *Chem. Rev.* **109**, 5755 (2009).
- ³⁵ B. J. Adzima, *Macromolecules* **41**, 9112 (2008).
- ³⁶ C. N. Bowman and C. J. Kloxin, *Angew. Chem. Int. Edit.* **51**, 4272 (2012).
- ³⁷ C. J. Kloxin, *Macromolecules* **43**, 2643 (2010).
- ³⁸ M. A. Tasdelen, *Polym. Chem.* **2**, 2133 (2011).
- ³⁹ R. J. Wojtecki, M. A. Meador, and S. J. Rowan, *Nat. Mater.* **10**, 14 (2011).
- ⁴⁰ T. Nakajima, N. Takedomi, and T. Kurokawa, *Polym. Chem.* **1**, 693 (2010).
- ⁴¹ Z. Tao, H. L. Fan, J. C. Huang, T. L. Sun, T. Kurokawa, and J. P. Gong, *ACS Appl. Mater. Inter.* **11**, 37139 (2019).
- ⁴² M. Ilyas, Md. A. Haque, Y. Yue, T. Kurokawa, T. Nakajima, T. Nonoyama, and J. P. Gong *Macromolecules* **50**, 8169 (2017).
- ⁴³ F. Luo, T. L. Sun, T. Nakajima, T. Kurokawa, Y. Zhao, K. Sato, A. B. Ihsan, X. Li, H. Guo, and J. P. Gong *Adv. Mater* **27**, 2722 (2015).

Tables caption

Table 1. Values of parameters used in equations (19) for the DN hydrogel with various amount of polymer chains involved in the mechanochemical reactions.

Table 2. Values of parameters used in equations (19) for PNaAMPS/PEA DN hydrogels.

Table 3. Values of parameters used in equations (19) for the yielding stress of DN hydrogels with various types of network component.

Table 4. Values of parameters used in equations (19) for the yielding stress of DN and PVA-DN hydrogels with 0.1 and 0.6 mol% of 2-oxoglutaric acid photoinitiator.

Table 5. Values of parameters used in equations (19) for different molar fraction $f_{\text{NBOC}} = 0.1, 0.15$ and 0.2 .

Figures caption

Figure 1. An illustration of Flory-Huggins lattice model for polymer chains immersed into a solvent, where there are mechanochemical reactions.

Figure 2. Schematic diagram of mechanochemical reaction of dynamic bonds and their Rouse diffusion motions.

Figure 3. Simulation results of stress as a function of elongation ratio for the DN hydrogel at a given $N_{ta}k_B T = -4$ MPa, 0 MPa, 4 MPa, 8 MPa and 12 MPa.

Figure 4. Comparison of simulation results and experimental data [18] for the stress as a function of elongation ratio of PNaAMPS/PEA DN hydrogels with a variety of molar concentrations of the PNaAMPS network.

Figure 5. Comparison of simulation and experimental results [18] for yielding stress as a function of elongation ratio of DN hydrogels with various network components.

Figure 6. Comparisons of simulation results and experimental data [40] for the yielding stress as a function of elongation ratio of DN and PVA-DN hydrogels with 0.1 and 0.6 mol% of 2-oxoglutaric acid photoinitiator.

Figure 7. Comparisons between numerical results using equation (19) and experimental data reported in Ref. [41] of the UM/NBOC hydrogels at a variety of molar fractions of the NBOC network of $f_{\text{NBOC}}=0.1, 0.15$ and 0.2 .